Research Article | Vol. 25, No. 17 | 21 Aug 2017 | OPTICS EXPRESS 19863
Optics EXPRESS

Broad tunable photonic microwave generation based on period-one dynamics of optical injection vertical-cavity surface-emitting lasers

SONGKUN JI,[1] YANHUA HONG,[1,*] PAUL S. SPENCER,[1] JOHANNES BENEDIKT,[2] AND IWAN DAVIES[3]

[1]*School of Electronic Engineering, Bangor University, Gwynedd LL57 1UT, Wales, UK*
[2]*School of Engineering, Cardiff University, Queen's Building, The Parade, Cardiff CF24 3AA, UK*
[3]*IQE plc, Cardiff CF3 0LW, Wales, UK*
**y.hong@bangor.ac.uk*

Abstract: Photonic microwave generation based on period-one dynamics of an optically injected VCSEL has been study experimentally. The results have shown that the frequency of the generated microwave signal can be broadly tunable through the adjustment of the injection power and the frequency detuning. Strong optical injection power and higher frequency detuning are favorable for obtaining a high frequency microwave signal. These results are similar to those found in systems based on distributed feedback lasers and quantum dot lasers. The variation of the microwave power at the fundamental frequency and the second-harmonic distortion have also been characterized.

OCIS codes: (140.7260) Vertical cavity surface emitting lasers; (140.5960) Semiconductor lasers; (060.5625) Radio frequency photonics; (350.4010) Microwaves.

References and links

1. N. Dagli, "Wide-bandwidth lasers and modulators for RF photonics," IEEE Trans. Microw. Theory Tech. **47**(7), 1151–1171 (1999).
2. S. C. Chan and J. M. Liu, "Tunable narrow-linewidth photonic microwave generation using semiconductor laser dynamics," IEEE J. Sel. Top. Quantum Electron. **10**(5), 1025–1032 (2004).
3. S.-C. Chan, S.-K. Hwang, and J.-M. Liu, "Period-one oscillation for photonic microwave transmission using an optically injected semiconductor laser," Opt. Express **15**(22), 14921–14935 (2007).
4. J. Capmany and D. Novak, "Microwave photonics combines two worlds," Nat. Photonics **1**(6), 319–330 (2007).
5. J. Yao, "Microwave photonics," J. Lightwave Technol. **27**(3), 314–335 (2009).
6. Y.-S. Juan and F.-Y. Lin, "Photonic Generation of Broadly Tunable Microwave Signals Utilizing a Dual-Beam Optically Injected Semiconductor Laser," IEEE Photonics J. **3**(4), 644–650 (2011).
7. C. Lim, A. Nirmalathas, D. Novak, R. Waterhouse, and G. Yoffe, "Millimeter-wave broad-band fiber-wireless system incorporating baseband data transmission over fiber and remote LO delivery," J. Lightwave Technol. **18**(10), 1355–1363 (2000).
8. D. Novak, R. B. Waterhouse, A. Nirmalathas, C. Lim, P. A. Gamage, T. R. Clark, M. L. Dennis, and J. A. Nanzer, "Radio-Over-Fiber Technologies for Emerging Wireless Systems," IEEE J. Quantum Electron. **52**(1), 0600311 (2016).
9. X.-Q. Qi and J.-M. Liu, "Photonic Microwave Applications of the Dynamics of Semiconductor Lasers," IEEE J. Sel. Top. Quantum Electron. **17**(5), 1198–1211 (2011).
10. T. B. Simpson, J. M. Liu, M. Almulla, N. G. Usechak, and V. Kovanis, "Linewidth sharpening via polarization-rotated feedback in optically injected semiconductor laser oscillators," IEEE J. Sel. Top. Quantum Electron. **19**(4), 1500807 (2013).
11. J.-P. Zhuang and S.-C. Chan, "Tunable photonic microwave generation using optically injected semiconductor laser dynamics with optical feedback stabilization," Opt. Lett. **38**(3), 344–346 (2013).
12. C. Cui, X. Fu, and S.-C. Chan, "Double-locked semiconductor laser for radio-over-fiber uplink transmission," Opt. Lett. **34**(24), 3821–3823 (2009).
13. L. Fan, G. Xia, J. Chen, X. Tang, Q. Liang, and Z. Wu, "High-purity 60GHz band millimeter-wave generation based on optically injected semiconductor laser under subharmonic microwave modulation," Opt. Express **24**(16), 18252–18265 (2016).
14. T. B. Simpson, J.-M. M. Liu, M. AlMulla, N. G. Usechak, and V. Kovanis, "Limit-cycle dynamics with reduced sensitivity to perturbations," Phys. Rev. Lett. **112**(2), 023901 (2014).

#292640 https://doi.org/10.1364/OE.25.019863
Journal © 2017 Received 11 Apr 2017; revised 28 Jul 2017; accepted 30 Jul 2017; published 8 Aug 2017

Optics EXPRESS

15. A. Hurtado, I. D. Henning, M. J. Adams, and L. F. Lester, "Generation of tunable millimeter-wave and THz signals with an optically injected quantum dot distributed feedback laser," IEEE Photonics J. **5**(4), 5900107 (2013).
16. S.-C. Chan, S.-K. Hwang, and J.-M. Liu, "Radio-over-fiber AM-to-FM upconversion using an optically injected semiconductor laser," Opt. Lett. **31**(15), 2254–2256 (2006).
17. C. Wang, R. Raghunathan, K. Schires, S.-C. Chan, L. F. Lester, and F. Grillot, "Optically injected InAs/GaAs quantum dot laser for tunable photonic microwave generation," Opt. Lett. **41**(6), 1153–1156 (2016).
18. C. H. Chang, L. Chrostowski, and C. J. Chang-Hasnain, "Injection Locking of VCSELs," IEEE J. Sel. Top. Quantum Electron. **9**(5), 1386–1393 (2003).
19. F. Koyama, "Recent Advances of VCSEL Photonics," J. Lightwave Technol. **24**(12), 4502–4513 (2006).
20. D. Parekh, X. Zhao, W. Hofmann, M. C. Amann, L. A. Zenteno, and C. J. Chang-Hasnain, "Greatly enhanced modulation response of injection-locked multimode VCSELs," Opt. Express **16**(26), 21582–21586 (2008).
21. A. Quirce, A. Valle, H. Lin, D. W. Pierce, and Y. Zhang, "Photonic generation of high-frequency microwave signals utilizing a multi-transverse-mode vertical-cavity surface-emitting laser subject to two-frequency orthogonal optical injection," J. Opt. Soc. Am. B **29**(12), 3259–3270 (2012).
22. A. Quirce and A. Valle, "High-frequency microwave signal generation using multi-transverse mode VCSELs subject to two-frequency optical injection," Opt. Express **20**(12), 13390–13401 (2012).
23. P. Perez, A. Quirce, A. Valle, A. Consoli, I. Noriega, L. Pesquera, and I. Esquivias, "Photonic generation of microwave signals using a single-mode VCSEL subject to dual-beam orthogonal optical injection," IEEE Photonics J. **7**(1), 5500614 (2015).
24. Y. Zhou, Z.-M. Wu, L. Fan, B. Sun, Y. He, and G.-Q. Xia, "Two channel photonic microwave generation based on period-one oscillations of two orthogonally polarized modes in a vertical-cavity surface-emitting laser subjected to an elliptically polarized optical injection," Wuli Xuebao **64**(20), 204203 (2015).
25. B. Sun, J.-G. Wu, S.-T. Wang, Z.-M. Wu, and G.-Q. Xia, "Theoretical and experimental investigation on the narrow-linewidth photonic microwave generation based on parallel polarized optically injected 1550 nm vertical-cavity surface-emitting laser," Wuli Xuebao **65**(1), 014207 (2016).

1. Introduction

Photonic generation of high-frequency microwave signals has gained much attention over the past decade [1–6]. One of the main motivations behind these studies is their potential application in radio-over-fiber (RoF) system. Compared with conventional circuitry based microwave generation, photonic microwave generation in RoF offers several advantages, such as, low cost, high speed, longer transmission distance, low power consumption and less system integration complexity [7,8]. Many photonic microwave generation techniques have been proposed, which includes direct modulation, optical heterodyne technique, external modulation, mode-locked semiconductor lasers, optoelectronic oscillator (OEO) and period one (P1) [9]. Among these techniques, photonic microwave generation based on P1 oscillation dynamic has gained much more attention in the recent studies due to the many advantages of this approach, such as: a nearly single sideband (SSB) spectrum, which minimizes the power penalty [3], low cost due to all-optical components configuration [10] and widely tunable oscillation frequency far from its original relaxation resonance frequency [3,11–13]. P1 oscillation is obtained when a stable locked laser experiences a Hopf bifurcation, which generates two dominant frequencies: one is generated from the optical injection while the other one is emitted near the cavity resonance frequency [14]. The frequency of photonic microwave generation based on P1 can be broadly tunable by changing the injection power or frequency detuning. The generated frequency can far exceed the relaxation oscillation frequency of the injected semiconductor laser. Photonic microwave generation based on P1 oscillation has been investigated extensively in conventional single mode distributed feedback (DFB) laser [14,15]. The results show that 100 GHz with tuning range of tens of gigahertz photonic microwave signal can be achieved using P1 oscillation in DFB lasers [16]. Recently, a tunable photonic microwave with continuous tuning of the frequency up to 20 GHz has also been achieved experimentally in a quantum dot (QD) laser based on P1 oscillation [17].

To the best of our knowledge, there is no commercial available QD laser lasing around 1.55 μm and the wavelength region near 1.55 μm is the most popular for fiber communication systems due to its lowest optical attenuation. The DFB laser constitutes the majority cost of microwave generation based on P1 oscillation scheme, and the cost of a single-mode vertical-

Optics EXPRESS

cavity surface-emitting laser (VCSEL) is about one tenth of the price of a DFB laser. VCSELs also have many impressive characteristics, such as, low threshold current, low power consumption, circular beam profile, single-longitudinal mode operation, ease of fabrication and longevity. VCSELs subject to optical injection share many similar nonlinear dynamics as those in DFB lasers. The use of off-the-shelf VCSELs therefore offers a method to achieve low-cost and low power consumption of photonic microwave generation. In recent years, photonic microwave generation using VCSEL has drawn a great deal of attention [18–23]. More than 20 GHz photonic microwave signal has been obtained using dual-beam orthogonal optical injected in a single-transverse-mode VCSEL [23], however, no significant reduction of the linewidth is achieved by using double injection because the linewidth is mainly determined by the phase fluctuations of the two master lasers. An invited paper [9] has reported that photonic microwave generation based on P1 oscillation has many advantages compared with the other proposed techniques, including simple electronics, tunability and single sideband. Two channel photonic microwave generation based on P1 of two orthogonally polarized modes in a VCSEL subjected to an elliptically polarized optical injection has also been numerically simulated and analyzed [24]. 30GHz microwave signal have also been observed in parallel-polarized optical injection in VCSEL with the injection wavelength close to the suppressed polarized mode [25]. The generated microwave frequency in [25] is dependent on the frequency different between the dominant mode and the suppression orthogonal mode. The frequency difference between the dominant mode and the suppression orthogonal mode is induced by anisotropies of the VCSEL materials, which is difficult to control during device fabrication. As such the photonic microwave generation using this method provide less feasibility of selection of the microwave frequency. In this paper, we have experimentally investigated the photonic microwave signal generation using low-cost off-the-shelf single mode VCSELs based on similar physical mechanism reported in DFB laser [14,15] in order to achieve the low cost and low power consumption of tunable photonic microwave generation. To the best our knowledge, no experimental confirmation of photonic microwave signal generation in VCSEL based on this scheme has been reported. The effect of the injection power and frequency detuning on the frequency of photonic microwave signal has been investigated. More than 15 GHz (due to limitation of the measured instruments) with tunability of more than 10 GHz photonic microwave signal has been demonstrated.

The remainder of this paper is organized as follows. The experimental setup is described in Section 2, followed by the experimental results in section 3. In section 4, we summarize the results obtained.

2. Experimental setup

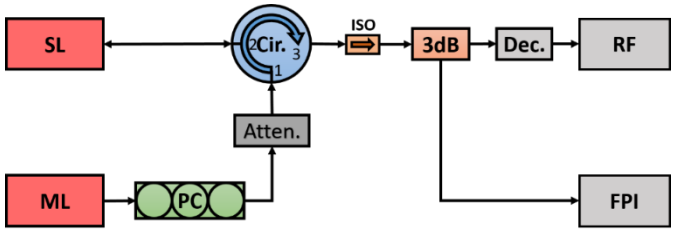

Fig. 1. The experimental setup. ML: Master laser, SL: Slave laser, PC: polarization controller, Atten: digital attenuator Cir: Optical circulator. ISO: optical isolator, 3dB: 2 by 2 3dB fiber coupler, Dec: photodetector, RF: radio frequency spectrum analyzer. FPI: Fabry-Perot interferometer.

Figure 1 shows the schematic experimental setup. It is all fiber setup. A commercial single-mode VCSEL (Raycan RC33xxx1F pigtail) was used as slave laser (SL). The VCSEL was driven by extra-low noise current and the temperature was control at 21.0 °C. At this temperature, the threshold current of the VCSEL was 1.3mA and its lasing wavelength was

Optics EXPRESS

1529.92nm at the bias current of 5mA. A tunable laser (TUNICS-BT 1550) with maximum output power of 10 mW and linewidths of 1 MHz was used as the master laser (ML). The output of the ML travelled through a polarization controller (PC), a digital fiber attenuator and an optical circulator, and injected into the slave laser. The polarization controller was used to control the polarization of the injection beam to be parallel to the slave laser's polarization direction; the attenuator was in place to adjust the injection power. The total output of the SL was split to two detection paths. One path was detected by 12GHz bandwidth photo-detectors (New Focus 1554-B) and recorded by a 30GHz RF spectrum analyzer (Anritsu MS 2667C); another path was sent to a Fabry-Perot interferometer (FPI). The output beam from the FPI was detected by a detector and sent to an oscilloscope (Tektronix TDS7404) for monitoring the optical spectra of the SL. The finesse of the FPI is 150 and the free spectrum range of the FPI was set at 19.9 GHz, so the resolution of the FPI was 0.133GHz. In this experiment, no polarization-resolved VCSEL's output was measured.

3. Experimental results

The VCSEL used in the experiment was a single transverse mode laser lasing at one linear polarization (X-polarization) near the threshold current. When the bias current was increased to 3.1 mA, the polarization switched to its orthogonal polarization (Y-polarization). Further increases in the bias current to 6.7 mA, see the polarization switch back to X-polarization and remained in this polarization until the bias current reached 9.3 mA. The frequency of X-polarization is about 5.1 GHz higher than that of Y-polarization at the polarization switching current. In the experiment, the bias current was fixed at 8.5 mA, unless stated elsewhere. The injection power was varied from 0.0007 mW to 1.86 mW and the frequency detuning was varied from –14.37GHz to + 13.32GHz. The injection power was measure at port 2 of the optical circulator and the output power of the free running VCSEL was found to be 1.70mW. The actual injection powers in the VCSEL were smaller than the measurement due to coupling loss. However, the quantity analysis on the effect of the injection power on the frequency of the generated photonic microwave is out of the scope of this paper. Therefore only the relative analysis was provided. The frequency detuning was calculated as $f_{ML} - f_{SL}$, where f_{ML} and f_{SL} are the frequencies of the ML and SL, respectively. The change of the frequency detuning is achieved by tuning the frequency of the ML. The VCSEL was operated at P1 dynamics for most of setting parameters.

3.1 Fundamental microwave frequency

Figure 2 presents the RF spectra of the VCSEL at several injection conditions under P1 oscillation. Figure 2(a) shows the spectrum of the VCSEL subject to optical injection with injection power of 0.37 mW and the frequency detuning of –2.9 GHz. The grey curve is the noise curve. It is very clear that the noise floor of the spectrum increases sharply at 8 GHz and above. This is because the RF spectrum analyzer uses different harmonic orders of the mixer for different frequency ranges. For the 0–8.1 GHz frequency range, the first harmonic order of the mixer has been used; for 8.0–15.3 GHz frequency range, the second harmonic order of the mixer has been used. As a result, the noise level is increased for the frequency of 8.00 GHz. The output spectrum of the VCSEL in Fig. 2(a) indicates that the VCSEL is in P1 oscillation state with a fundamental frequency f_0 of 5.87 GHz. The optical spectrum of P1 oscillation in optical injection VCSEL contains a regenerative component at injection frequency fi and sidebands equally separated by the fundamental frequency of photonic microwave f_0 [9]. The beating between the regenerated mode and the second strongest sideband induces the second harmonic at $2f_0$, which has also been observed with power suppression of 20 dB in comparison with that at the fundamental frequency. Under the same frequency detuning, increasing the injection power to 0.74mW, see the generated microwave

Optics EXPRESS

frequency increase to 7.22 GHz, as shown in Fig. 2(b), which demonstrates that the injection power affects the fundamental frequency of the generated photonic microwave.

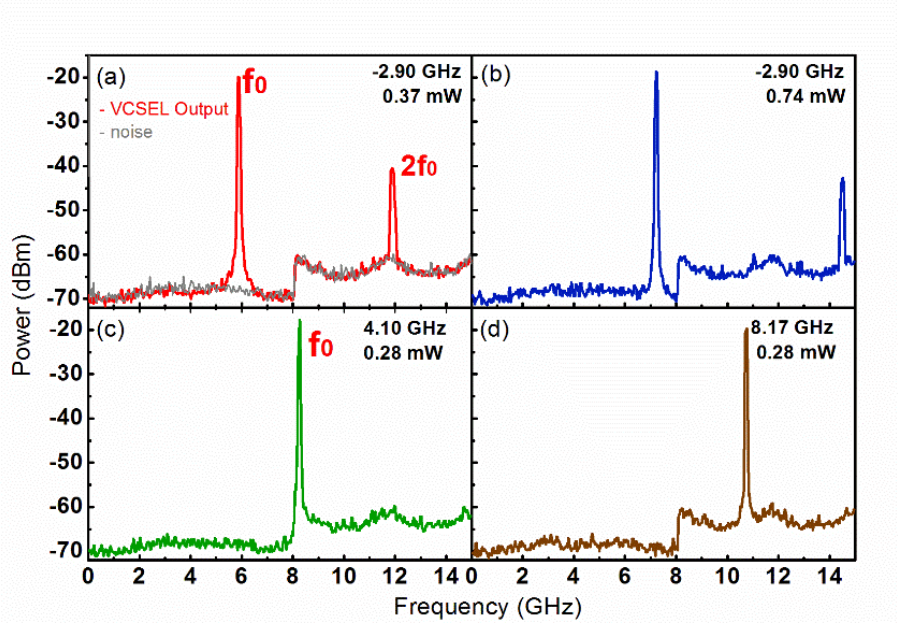

Fig. 2. The power spectra of the VCSEL output at injections frequency detuning and injection power of (a) (–2.9 GHz, 0.37mW), (b) (–29. GHz, 0.74 mW), (c) (4.1 GHz, 0.28 mW), (d) (8.17 GHz, 0.28 mW).

To observe the effect of frequency detuning on the fundamental frequency, we fix the injection power and varied the frequency detuning. Figures 2(c)-2(d) show the power spectra of the VCSEL with injection power of 0.28 mW and the frequency detuning of + 4.1 GHz and 8.17 GHz, respectively. In Fig. 2(c), 8.26 GHz of the fundamental frequency has been observed. At this operating parameters, we believe the second harmonic appeared at around 16.5 GHz, however, due to the detector bandwidth limitation, this second harmonic peak cannot be detected. Increasing the frequency detuning to 8.17 GHz, as shown in Fig. 2(d), the fundamental frequency increased to 10.74 GHz, which also indicate the fundamental frequency related to the frequency detuning in this P1 region.

The generated microwave fundamental frequency, f_0, variation as a function of frequency detuning under two different injection power is plotted in Fig. 3(a). The gap between the data lines are mostly injection locking (IL) with small P2 and chaos oscillation region. The VCSEL operated above Hopf bifurcation boundary for the curves at the right side of the gap and below saddle-node bifurcation boundary for the curves at the left side of the gap. When the injection power is small (black lines, injection power of 0.093mW), the frequency shift rate of f_0 is higher in the negative frequency detuning. Increasing the injection power to 0.558mW, causes the injection locking to shift to a more negative frequency detuning region. The results also show that the frequency shift rate for the injection power of 0.558 mW is lower than that for the injection power of 0.093 mW for the detuning frequencies above the Hopf bifurcation boundary.

Figure 3(b) displays the fundamental frequency f_0 as a function of the injection power with four fixed frequency detunings. The results show that the frequencies f_0 increase monotonically with the increasing injection power. For lower injection powers (<0.5 mW), the frequency shift rates are varied for the different frequency detuning. The frequency shift

Optics EXPRESS

rates decreases with increasing frequency detuning. For the higher injection powers (>0.5 mW), the frequency shift rates are approximately constant for all detuning frequencies. This result is similar to that reported in DFB laser based configurations [3].

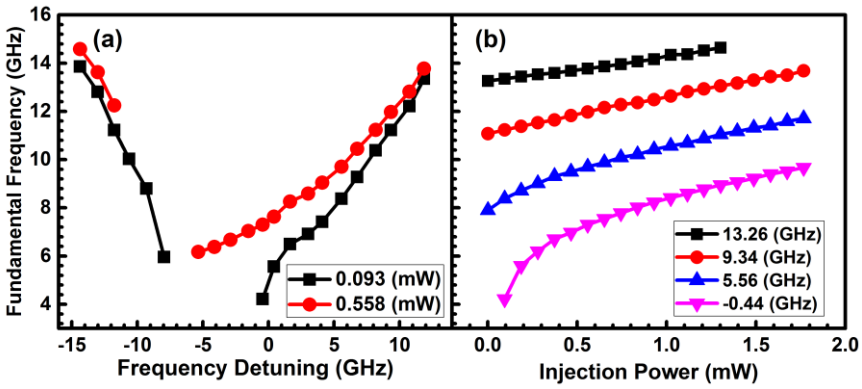

Fig. 3. Generated microwave frequency as function of (a) frequency detuning and (b) injection power.

The same physical mechanism in [3] can be used to explain the results observed in our VCSEL based system. Since the fundamental microwave frequency is the result of the frequency beating between the injection beam and the carrier frequency. When the VCSEL is subjected to optical injection, the carrier frequency experiences a red shift due to the increase of the refractive index and the pulling effect. The competition between the red-shifting and pulling effect induces the frequency shift rate change under different injection power and detuning frequency conditions.

A map of the generated microwave frequency for various detuning frequencies and injection powers is presented in Fig. 4, the two rainbow colored denote areas that exhibit period one dynamics. Injection locking, period-two and chaotic regions are embedded within the large grey area, which is not our focus in this paper. In the upper right corner of the black color areas, the oscillation frequencies are found to be outside of the measurement range of the instrumentation. The results in Fig. 4 indicate that the frequency detuning and the injection power greatly affect the frequency of photonic microwave. The frequency of photonic microwave signal increases with the increase of injection power, the frequency detuning above the Hopf bifurcation boundary and the absolute frequency detuning below the saddle node bifurcation boundary. The continuous tuning of the frequency from 4GHz to up to 15GHz due to the instruments limitation has been obtained.

Optics EXPRESS

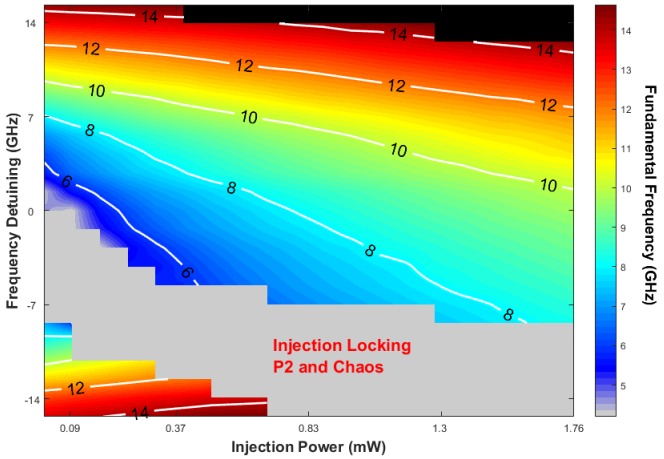

Fig. 4. Mapping of the fundamental frequency.

3.2 Microwave power

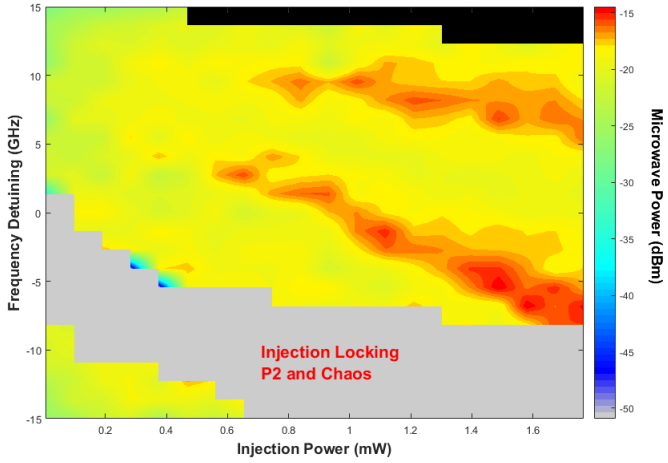

Fig. 5. Mapping of the fundamental microwave frequency power.

The optical frequency components are converted into microwave signals at the photo-detector. To utilize photonics generated microwave in RoF applications, it is important to understand how the power of the generated microwave varies with injection power and frequency detuning. As shown in Figs. 2(a)-2(b), the fundamental frequency f_0 and the second harmonic $2f_0$ can be observed at same time, the power at f_0 and $2f_0$ are denoted P_{f0} and P_{2f0}, respectively. Figure 5 maps the power P_{f0} at the fundamental frequency with the same injection conditions as those in Fig. 4. Similarly to Fig. 4, top right black area is out of our instrument detection range, the grey area is mainly the injection locking region and small P2 and Chaos regions. From the mapping, we can observe that the microwave power stays around −25dBm consistently over the whole frequency detuning range with P1 dynamics when injection power is below 0.2mW. Above injection powers of 0.2mW, the microwave P_{f0} increases to a power of around −20 dBm except in two areas (indicated with red color). The power in these two areas is approximate 4dB higher than in the adjacent

Optics EXPRESS

regions. These two areas have not been observed in DFB lasers [3] or quantum dot lasers [17]. The exactly physical mechanism is still not clear. This observation will be verified in the future studies and checked to see if it is specific to VCSELs.

In this study, we also characterize the second harmonic distortion (SHD) in the RF spectra of the generated microwave. The SHD is defined as the ratio of the second harmonic power P_{2f0} to the power at the fundamental frequency P_{f0} [17]. The SHD of the optically injected VCSEL is presented in Fig. 6. The frequency detuning range in this measurement is from −6 GHz to 4 GHz, which is smaller than those measurements for the microwave frequency. The reason is that the second harmonic peak is out of the detection range of the detector for the higher frequency detuning. Figure 6(a) shows that the SHD fluctuates around −27 dB for the injection power of 0.093 mW. No trend with the frequency detuning can be concluded. However, the SHD shows a tendency to decrease with the increasing frequency detuning within the measurement range for the injection powers of 0.279 mW and 0.465mW. These results have some similarity with the results in quantum dot laser [17], where the SHD is less sensitive to frequency detuning for low injection power. For intermedium injection powers, the maximum SHD was observed in the intermediate frequency detuning range in QD laser [17], however, this phenomenon has not been seen in our experiment. Figure 6(b) shows the SHD as a function of the injection power with three different detuning frequencies. The results show that the SHDs changes irregularly with the increasing injection power. No simple trend is observed. The weaker dependence of the SHD on the injection power seen in our experiment is similar to that reported in QD laser [17]. Lower amplitude fluctuations were observed at the most negative detuning frequency among these three detuning frequencies. The optical spectra of the VCSEL output have not been recorded, so we cannot describe the SSB characteristics of the generated photonic microwave. This will be studied in the future work.

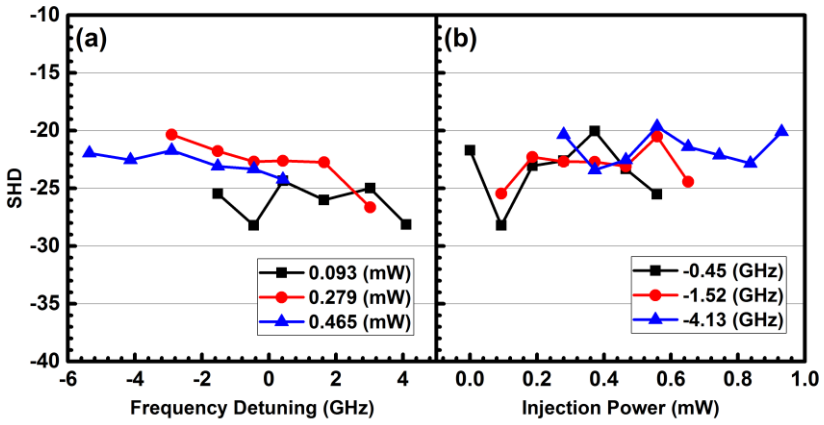

Fig. 6. Second harmonic distortion as a function of (a) the frequency detuning, (b) the injection power.

4. Conclusion

Photonic microwave generation based on P1 dynamics of a VCSEL subject to parallel injection has been studied experimentally. Continuous tuning of the microwave frequency from 4GHz to up to an instrumentation limited 15GHz was observed. Further increases the microwave frequency are possible by increasing the injection power or the frequency detuning. It has demonstrated that the frequency of the generated microwave increases with increasing frequency detuning above the Hopf bifurcation boundary and increasing injection power. The frequency detuning has little influence on the power of the generated microwave

Optics EXPRESS

except two small areas. On the other hand, the SHD decreases with increasing frequency detuning for higher injection power. The injection power has some effect on the power of the generated microwave signal, however, it has very limited effect on the SHD. This study underlines the potential of using low-cost off-the-shelf VCSELs to realize widely tunable photonic microwave oscillators based on period one oscillation.

Funding

The Sêr Cymru National Research Network in Advanced Engineering and Materials (NRN158).